YMTHE, Volume *30*

Supplemental Information

Gene editing in a *Myo6* semi-dominant mouse model rescues auditory function

Yuanyuan Xue, Xinde Hu, Daqi Wang, Di Li, Yige Li, Fang Wang, Mingqian Huang, Xi Gu, Zhijiao Xu, Jinan Zhou, Jinghan Wang, Renjie Chai, Jun Shen, Zheng-Yi Chen, Geng-Lin Li, Hui Yang, Huawei Li, Erwei Zuo, and Yilai Shu

Supplemental Information

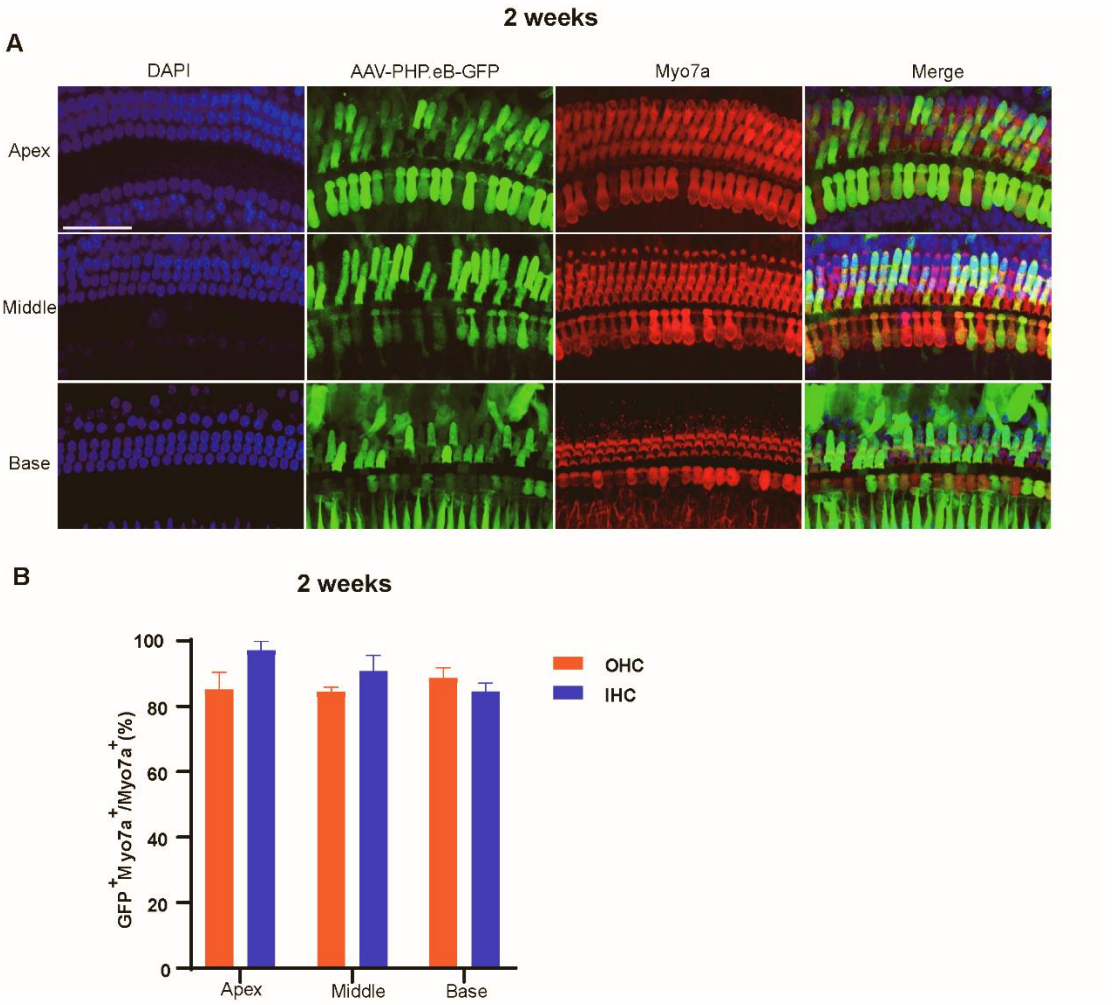

Figure S1. Infection efficiencies of AAV.PHP.eB-GFP for hair cells *in vivo* at 2 weeks.
(A) The AAV.PHP.eB-GFP viruses were packaged and injected into the cochleae of P0-2 mice. The AAV.PHP.eB-GFP-treated cochleae were dissected for immunostaining at 2 weeks post-injection. The apical, middle, and basal turns were dissected and stained with MYO7A (red) for hair cells and with DAPI (blue) for nuclei. (B) Infection efficiencies of AAV-PHP.eB were measured as the percentage of GFP^+ cells in IHCs and OHCs. Results were obtained from three animals and are presented as the mean ± SEM. Scale bar, 50 μm.

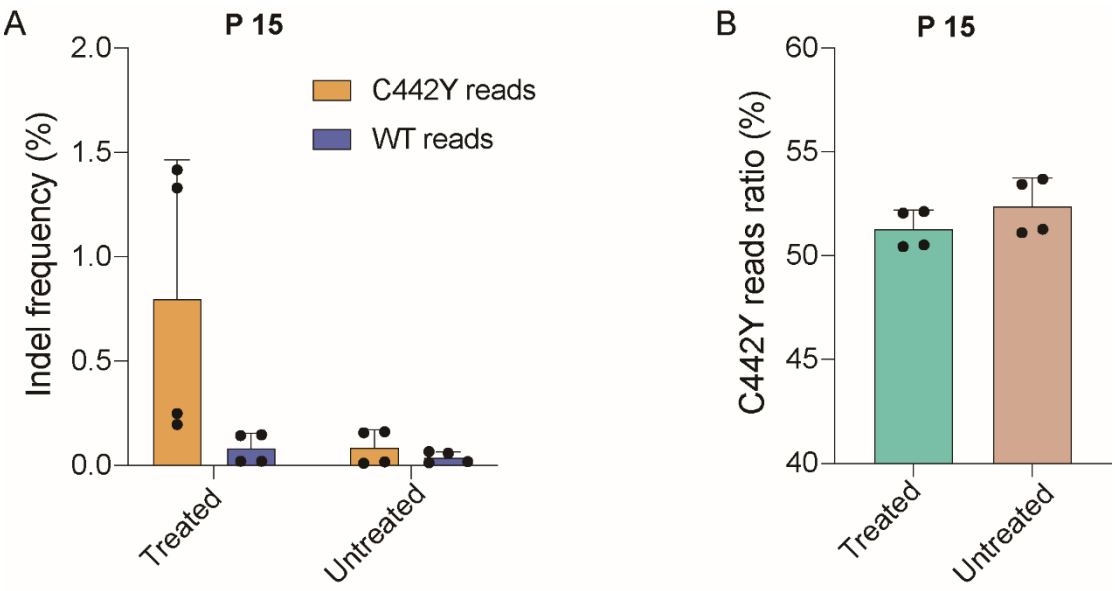

Figure S2. Gene editing efficiency analysis at the mRNA level using AAV.PHP.eB-SaCas9-KKH-Myo6-g2 *in vivo* at P15.

(A) The indel percentages at P15 in *Myo6*$^{WT/\ C442Y}$ whole cochlea at the mRNA level were determined by targeted NGS. To obtain mRNA from the cochlea, we extracted the whole cochlea soft tissue at P15, isolated RNA, reverse transcribed it to cDNA, and analyzed the cDNA by NGS. Each dot represents the mRNA from one AAV.PHP.eB-SaCas9-KKH-Myo6-g2-treated cochlea. Data are presented as the mean ± SD. (B) Relative read counts for *Myo6*^{C442Y} and *Myo6*^{WT} representing the mRNA in untreated and AAV.PHP.eB-SaCas9-KKH-Myo6-g2-treated cochleae at P15. Data are presented as the mean ± SD.

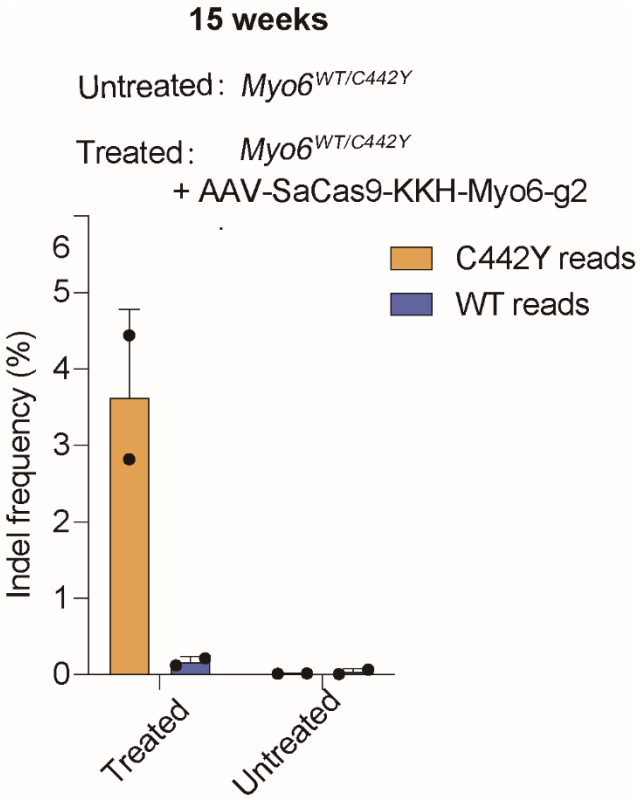

Figure S3. *In vivo* genome editing with the AAV.PHP.eB-SaCas9-KKH-Myo6-g2 at 15 weeks. The indel percentage at 15 weeks in *Myo6*$^{WT/C442Y}$ mice was determined by targeted NGS. The whole cochlea soft tissues were from *Myo6*$^{WT/C442Y}$ mice injected with AAV.PHP.eB-SaCas9-KKH-Myo6-g2 at P0-2 via the scala media (n = 2). Data are presented as the mean ± SD.

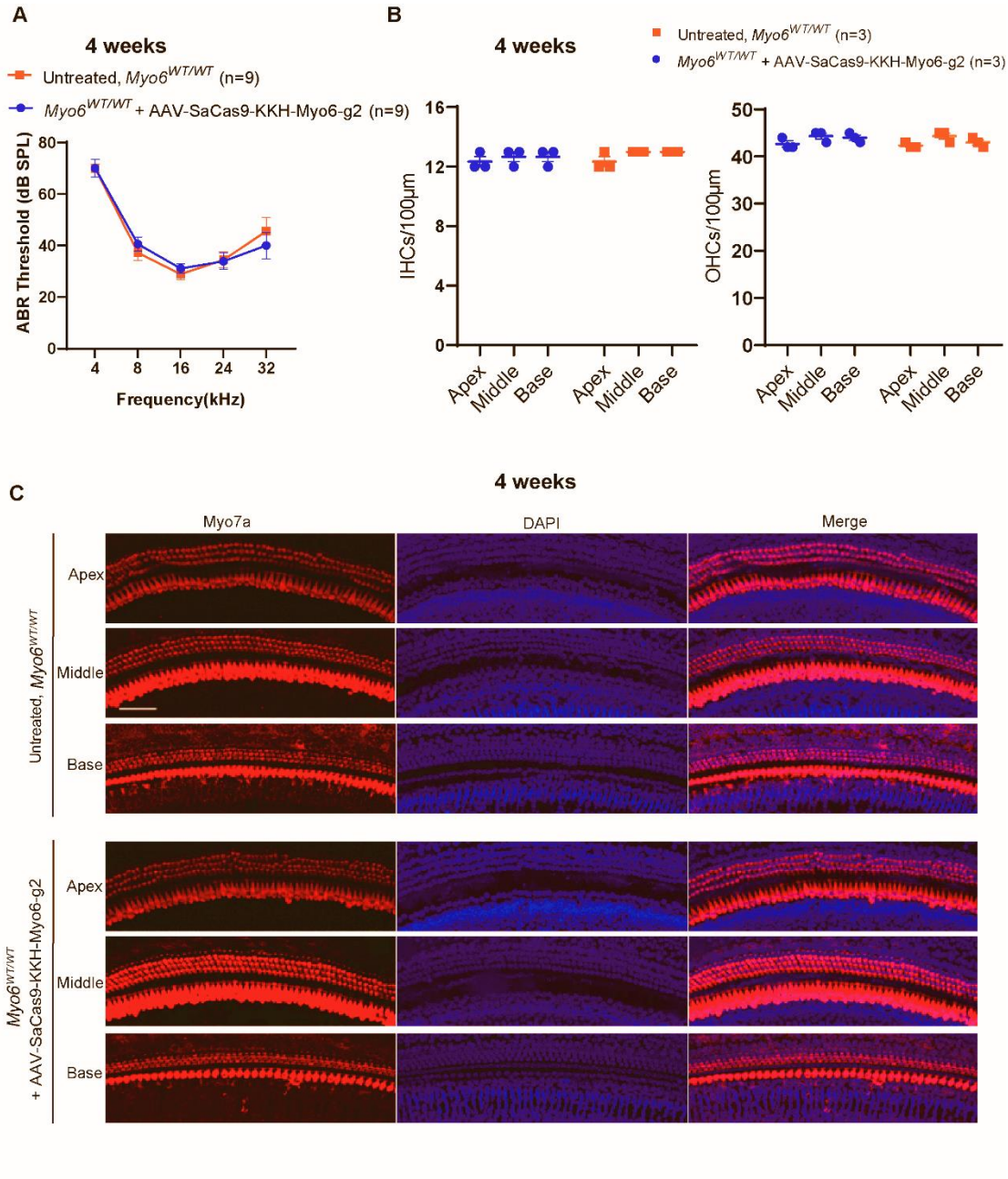

Figure S4. Effects of AAV.PHP.eB-SaCas9-KKH-Myo6-g2 on ABR thresholds of WT mice at 4 weeks. (A) ABR thresholds of AAV.PHP.eB-SaCas9-KKH-Myo6-g2-treated ears and the corresponding thresholds of their contralateral untreated ears. Audiometry measurements were conducted 4 weeks after AAV injection at P0-2. Values and error bars reflect the mean ± SEM. Statistical analysis was by two-tailed Student's *t*-tests. A *P*-value of less than 0.05 was considered significant. (B) The numbers of IHCs (left) and OHCs (right) per 100-μm section for three untreated and three AAV.PHP.eB-SaCas9-KKH-Myo6-g2-treated *Myo6*$^{WT/WT}$ mice. Values and error bars reflect the mean ± SEM. Statistical analysis was by two-tailed Student's *t*-tests. A *P*-value of less than 0.05 was considered significant. (C) Representative immunostaining images of hair cells in the untreated and AAV.PHP.eB-SaCas9-KKH-Myo6-g2-treated *Myo6*$^{WT/WT}$ cochleae at 4 weeks after injection. Scale bar, 50 μm.

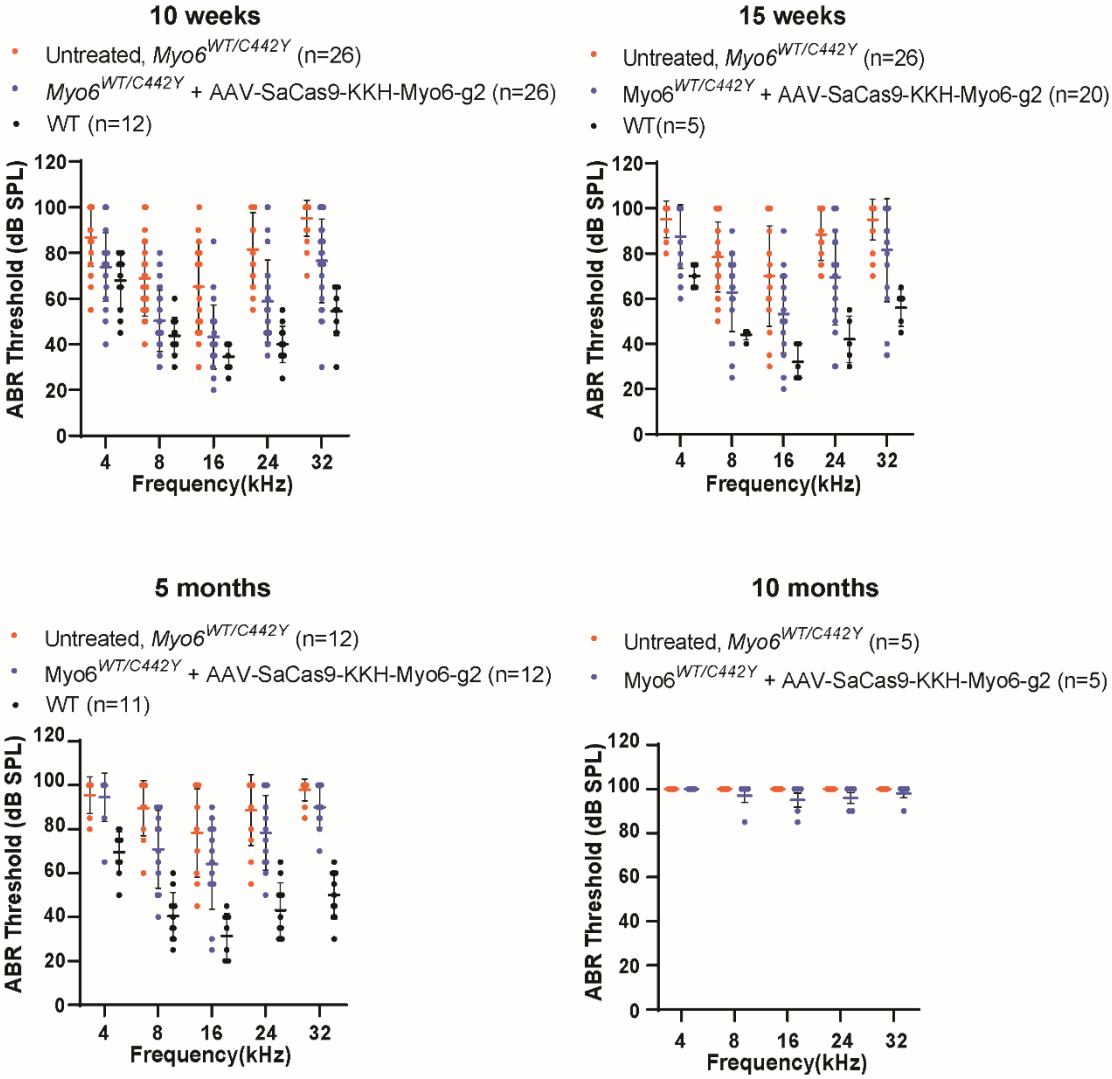

Figure S5. The hearing thresholds of individual mice at 10 weeks, 15 weeks, 5 months, and 10 months.

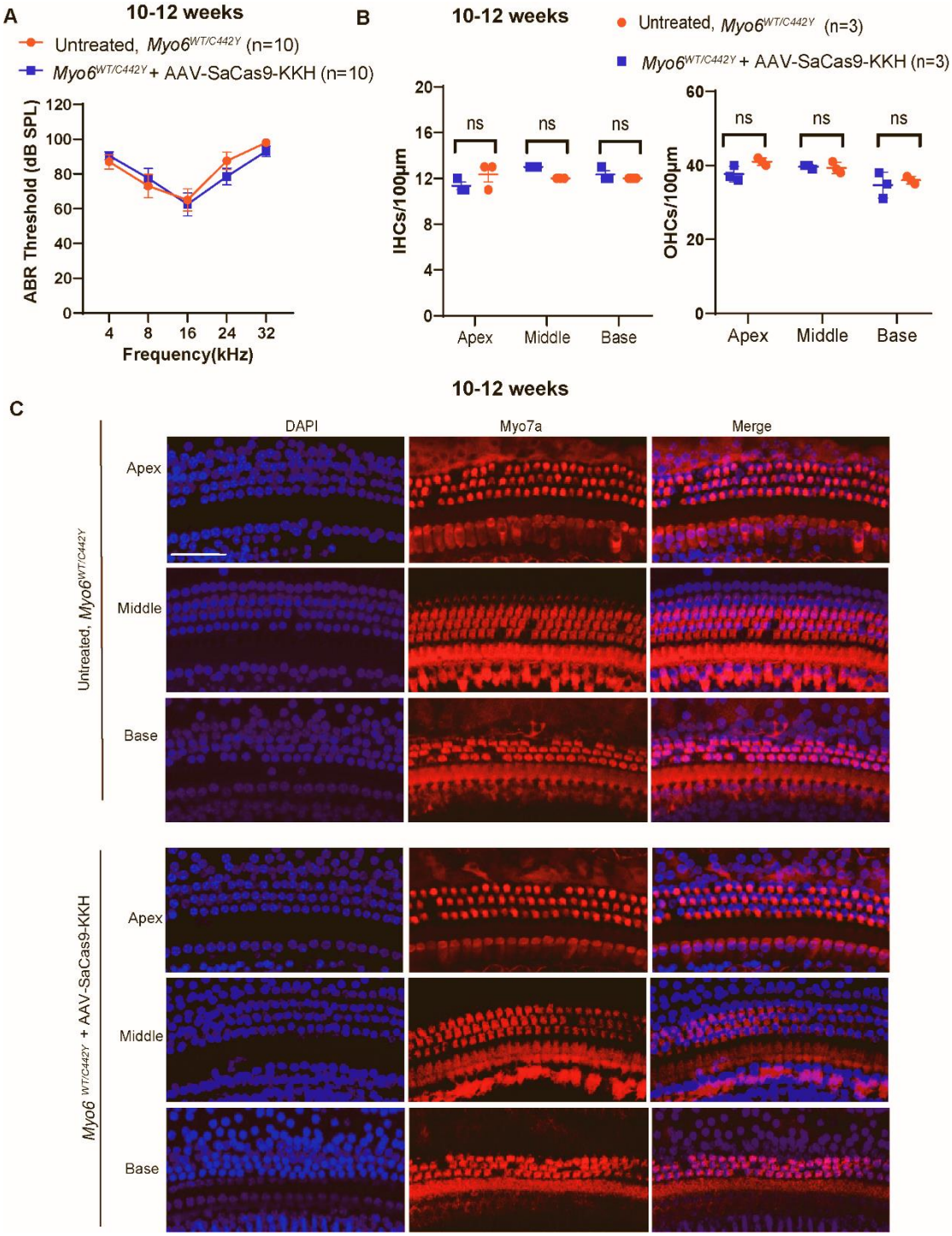

Figure S6. ABRs and confocal images of the AAV.PHP.eB-SaCas9-KKH-treated and untreated *Myo6*$^{WT/C442Y}$ mouse model at 10-12 weeks. (A) ABR thresholds of AAV.PHP.eB-SaCas9-KKH-treated *Myo6*$^{WT/C442Y}$ ears with the corresponding thresholds of their contralateral untreated ears. Audiometry measurements were conducted in 10–12-week-old mice that were treated with AAV.PHP.eB-SaCas9-KKH at P0-2. Values and error bars reflect the mean ± SEM. Statistical analysis was by two-tailed Student's *t*-tests. A *P*-value of less than 0.05 was considered significant. (B) The numbers of IHCs (left) and OHCs (right) per 100-μm section for three untreated and AAV.PHP.eB-SaCas9-KKH-treated *Myo6*$^{WT/C442Y}$ mice. Values and error bars reflect the mean ± SEM. Statistical analysis was by two-tailed Student's *t*-tests. A *P*-value of less than 0.05 was considered significant. (C) Representative immunostaining images of hair cell infection in the untreated and AAV.PHP.eB-SaCas9-KKH-treated *Myo6*$^{WT/C442Y}$ cochleae at 10-12 weeks after injection. Scale bar, 50 μm.

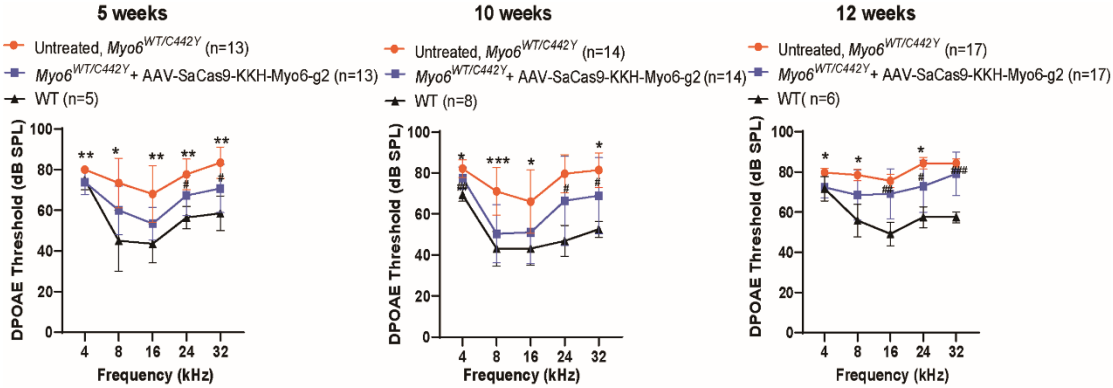

Figure S7. Effects of AAV.PHP.eB-SaCas9-KKH-Myo6-g2 on DPOAE thresholds in *Myo6*$^{WT/C442Y}$ mice. Comparison of DPOAE thresholds from untreated and AAV.PHP.eB-SaCas9-KKH-Myo6-g2-treated *Myo6*$^{WT/C442Y}$ ears at 5, 10, and 12 weeks. Statistical analysis between untreated and AAV.PHP.eB-SaCas9-KKH-Myo6-g2-treated *Myo6*$^{WT/C442Y}$ ears was by one-way ANOVA: ***$p < 0.001$; **$p < 0.01$; *$p < 0.05$. The statistical analysis between wild type and AAV.PHP.eB-SaCas9-KKH-Myo6-g2-treated *Myo6*$^{WT/C442Y}$ ears was by one-way ANOVA: ###$p < 0.001$; ##$p < 0.01$; #$p < 0.05$. Values and error bars reflect the mean ± SD.

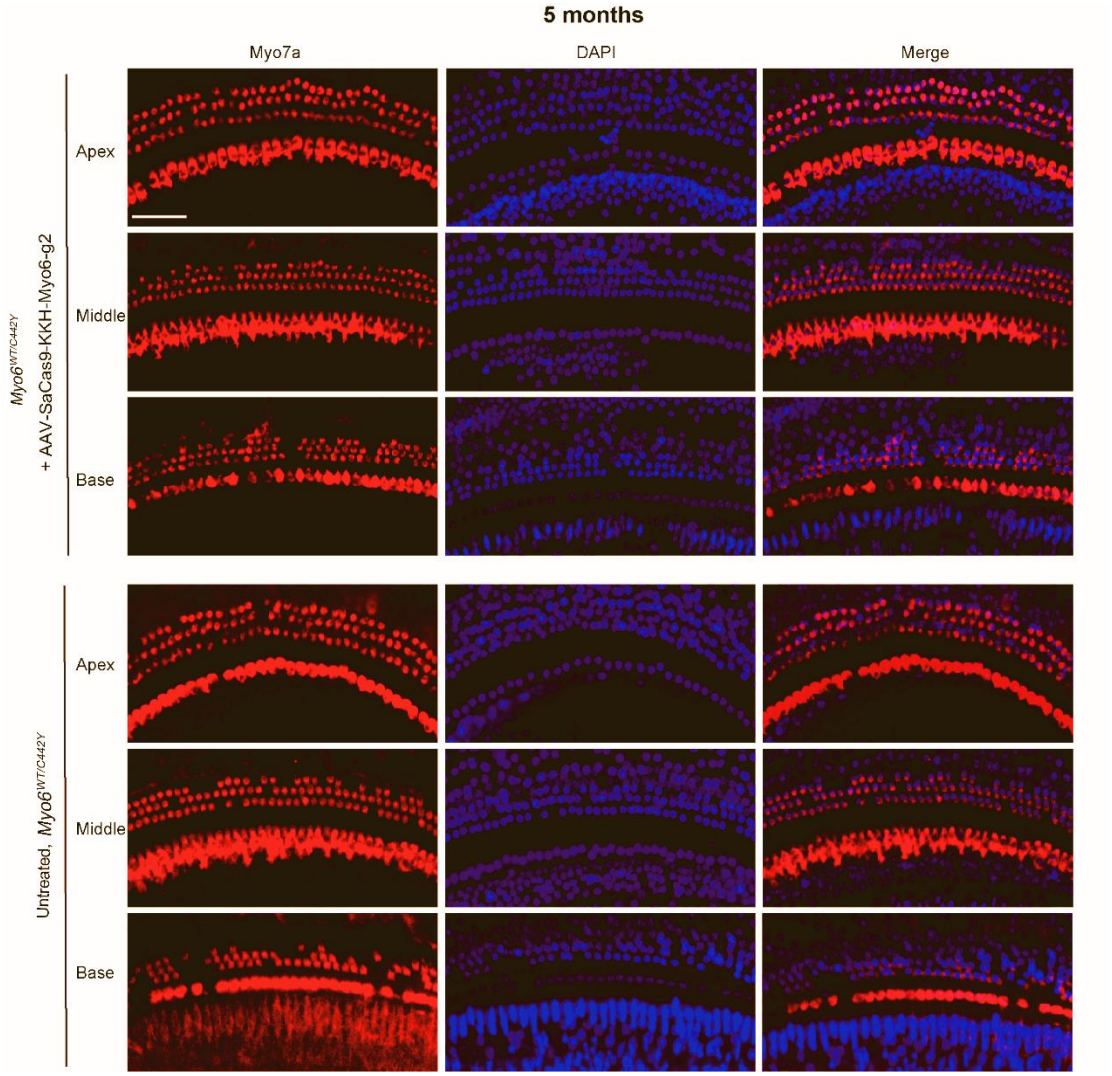

Figure S8. Representative confocal images of cochleae harvested at 5 months from the AAV-PHP.eB-SaCas9-KKH-g2 untreated and treated ears of *Myo6*$^{WT/C442Y}$ mice. The apical, middle, and basal turns were dissected and stained with MYO7A (red) for hair cells and with DAPI (blue) for nuclei. Scale bar, 50 μm.